HXT Observations of Solar Flares — A Review and Perspective —

Taro Sakao
National Astronomical Observatory, Mitaka, Tokyo 181-8588, Japan
E-mail: sakao@solar.mtk.nao.ac.jp

Abstract

We present hard X-ray imaging observations of impulsive solar flares made with the Hard X-ray Telescope (HXT) aboard the *Yohkoh* satellite, and emphasise the magnetic field structure and its evolution during flares. The HXT has revealed that the bulk of hard X-rays above 30 keV is emitted from the footpoints of a flaring magnetic loop by electrons accelerated near the loop top. This implies that the evolution of hard X-ray footpoints reflects that of magnetic field structure responsible for the energy release, through which we can infer the magnetic field structure itself.

We review progress so far made along these lines, including the relationship between magnetic field structure and thermal/non-thermal aspects of impulsive flares, followed by discussion of the (three-dimensional) magnetic field structure inferred from motions of individual footpoints. We also discuss, from a viewpoint of magnetic field structure, near-future perspective of hard X-ray solar physics.

Key words: Sun: flares — Sun: activity — Particle acceleration — Sun: X-rays

1. Introduction

Hard X-rays from solar flares contain wealth of information on acceleration and propagation of energetic electrons. The accelerated electrons, which are believed to contain a significant fraction (as high as half) of the total energy released in a flare, emit hard X-rays as they interact with ambient plasmas. Since the corona is optically thin to hard X-rays and they propagate without being affected by the magnetic field, hard X-ray observations of flares are expected to provide us with direct clues for investigating high energy processes which take place in flares.

Since the beginning of observations in October 1991, the Hard X-ray Telescope (HXT; Kosugi *et al.*, 1991) aboard the *Yohkoh* satellite (Ogawara *et al.* 1991) has observed more than 1,300 flares. The HXT is designed to image hard X-ray sources of solar flares in the energy range covering 14 to 93 keV in four bands (14-23-33-53-93 keV), with angular and temporal resolutions as high as $\sim 5''$ and 0.5 seconds, respectively. It should be stressed that the HXT has provided, for the first time, hard X-ray images of solar flares above 30 keV where little contamination is expected from hot plasmas ($T_{\rm e} \gtrsim$ 20 MK) created during the course of flares.

With these advanced capabilities over its predecessors (*Hinotori* SXT and *SMM* HXIS), the HXT has thus far revealed various fundamental characteristics of hard X-ray emission in flares (see, *e.g.*, Kosugi *et al.* 1992 and Kosugi 1996 for reviews of HXT observations). The most remarkable finding so far made with HXT is the discovery of the so-called above-the-loop-top impulsive hard X-ray source by Masuda (Masuda 1994; Masuda *et al.* 1994; Masuda *et al.* 1995). By analyzing several impulsive flares which commenced near the solar limb (*e.g.*, the 13 January 1992 flare), Masuda has found that there appears an impulsive hard X-ray source (in the energy range $\gtrsim$ 30 keV) situated *above* the corresponding soft X-ray loop imaged with *Yohkoh* SXT (Soft X-ray Telescope; Tsuneta *et al.* 1991). This discovery has clearly demonstrated that something energetic is taking place outside the closed magnetic lines of force. It has long been postulated that energy release associated with X- (or Y-) type magnetic reconnection which progresses at the tip of a cusp-shaped magnetic field, with closed field lines below it, could be responsible for Hα two ribbon events and post-flare loops (Hirayama 1974; Kopp and Pneuman 1976; Švestka *et al.* 1987; Schmieder *et al.* 1987; Forbes and Malherbe 1991), in long duration events (LDEs; Tsuneta *et al.* 1992a; Tsuneta 1996), and in soft X-ray arcade formation (Tsuneta *et al.* 1992b). The discovery of the above-the-loop-top impulsive hard X-ray source has indicated that this type of magnetic reconnection in the loop-with-a-cusp-shaped magnetic field is indeed taking place even in (at least some) impulsive flares, with much smaller temporal and spatial scales than those mentioned above.

In the meantime, observations of impulsive flares with HXT has revealed (Sakao 1994) that (1) the bulk of hard X-rays above 30 keV is emitted from the footpoints of flaring magnetic loop(s), manifesting itself most frequently as double sources located on either side of a magnetic neutral line, and (2) the double sources emit hard X-rays simultaneously, within a fraction of a second. This strongly suggests that the hard X-rays are emitted by electrons accelerated near the top of the loop, streaming down towards both ends. These characteristics, in turn, imply that hard X-ray double footpoint sources can be a powerful tool in investigating magnetic field structure responsible for the energy release. Immediately after departing the acceleration region in the corona, energized electrons precipitate along the flaring loop and emit hard X-rays at the footpoints (as long as the effect of magnetic mirroring is small), losing their energy instantaneously via the thick-target interaction. Hence, spatial evolution of hard X-ray footpoints may reflect nearly instantaneous evolution of the acceleration region in the corona, from which structure of the flaring magnetic field can be inferred. For example, for the loop-with-a-cusp configuration, energy release is expected to take place at higher altitudes in the corona as the flare progresses, resulting in a systematic increase in the separation between the double sources.

In this *manuscript*, we concentrate on recent findings on the structure of flaring magnetic field and related issues obtained by using the method described above. In section 2, we investigate magnetic field structure for impulsive flares inferred from temporal behavior of the separation of a pair of double footpoint sources, present a conjecture which includes relationship between the magnetic field structure and the creation of super-hot plasmas during the impulsive phase. (The reader is also referred to Sakao, Kosugi, and Masuda (1998) for detailed descriptions on this issue.) We further study in section 3 individual motions of each of a pair of hard X-ray double sources, compare them with the corresponding soft X-ray and Hα images, and discuss (three-dimensional) magnetic field structure responsible for the flare. In section 4, we discuss progress which is expected in the near-future as a direct extension of the investigation presented in this *manuscript*.

2. Magnetic Field Structure of Flares and their Thermal/Non-Thermal Characteristics

2.1. Event Selection and Method of Analysis

To investigate evolution of hard X-ray footpoint sources, we have selected 14 impulsive flares which show hard X-ray ($\gtrsim$ 30 keV) double footpoint sources during the impulsive phase. The event selection has been carried out based on the following criteria: (1) Events observed with HXT between October 1991 (*i.e.*, beginning of HXT observations) and December 1994. (2) Peak count rate in the M2-band exceeding 30 cts/s/SC (where SC stands for subcollimator each of which samples independent spatial Fourier component). (3) Double sources are clearly seen in the M2-band of HXT (33 – 53 keV) at the peak time of M2-band hard X-ray emission. The selected events are summarized in Table 1.

For the selected 14 flares, we have carried out a Gaussian fitting procedure (Sakao 1994) which provides centroid positions $(x_{\rm A}(t), y_{\rm A}(t))$ and $(x_{\rm B}(t), y_{\rm B}(t))$, together with their errors, for a pair of double sources A and B at each time t. In this section, we investigate the temporal behavior of the separation of the double sources which is given as follows:

$$s(t) = \sqrt{(x_{\rm A}(t) - x_{\rm B}(t))^2 + (y_{\rm A}(t) - y_{\rm B}(t))^2} \ . \tag{1}$$

Note that this quantity is free from spacecraft jitter. Figure 1 shows an example of events which show increasing footpoint separation (15 November 1991). We see that the separation of the double sources $s(t)$ shows repeated episodes of increase and decrease, while the overall separation increasing during the impulsive phase. The average separation velocity, $v_{\rm sep}$, during the time interval analyzed (22:37:32 UT – 22:38:08 UT) is 58.0 ± 3.7 km/s (corrected for foreshortening effects on the solar surface).

The separation velocity of the double sources for the 14 events are summarized in Table 1. We see in 7 out of the 14 events (events 1, 3, 4, 11 – 14), the double sources show significant increase in separation ($v_{\rm sep} > 0$; above the 3σ level) while the rest show either only marginal or even decreasing separation ($v_{\rm sep} \lesssim 0$).

2.2. Footpoint Separation and Spectral Characteristics

The behavior of the double sources, *i.e.*, whether they separate or not during the impulsive phase, has close relationship with the shape of the spatially integrated hard X-ray spectrum of the event. Figure 2 shows the relationship between $v_{\rm sep}$ (corrected for foreshortening effects) and $\Delta\gamma \equiv \gamma_{\rm M1/L} - \gamma_{\rm M2/M1}$, where $\gamma_{\rm M1/L}$ is the (single) power-law photon index obtained from M1- and L-band count data pair at the peak time of M2-band hard X-ray emission, and likewise for $\gamma_{\rm M2/M1}$. We see that events with increasing footpoint separation tend to show

Table 1. Double-footpoint separation velocity.

No.	Flare (UT)[1]		Hα Loc.	GOES/Hα	M2[2]	τ (s)[3]	v_{sep} (km/s)[4]	Note
1	91/11/02	06:45:45	S14W62	M9.1/1B	251	58.0	126.8 ± 8.4	
2	91/11/10	06:48:34	S14E56	M2.2/2B	151	14.0	–35.8 ± 30.7	(a), (c)
3	91/11/15	22:37:50	S14W19	X1.5/3B	528	35.5	58.0 ± 3.7	
4	91/12/03	16:36:17	N17E72	X2.2/2B	502	44.0	67.7 ± 22.4	
5	91/12/04	17:43:24	N17E58	M4.1/SN	36	82.0	–7.3 ± 12.9	
6	91/12/16	04:56:07	N04W45	M2.7/SF	154	15.0	–71.4 ± 25.5	(a)
7	92/02/07	11:54:29	S21W53	M3.7/2B	35	42.0	17.8 ± 16.7	
8	92/02/15	21:29:40	S16W13	M5.5/1B	33	32.0	7.8 ± 22.4	
9	92/09/10	22:52:26	N12E41	M3.2/2B	138	22.0	–0.1 ± 16.6	(b)
10	93/03/11	15:15:12	S04W34	M1.1/SF	82	25.0	–15.2 ± 27.0	(a)
11	93/04/22	14:08:26	N11E04	M1.5/SB	75	32.0	91.3 ± 13.4	
12	94/01/27	05:09:17	N11W65	M2.7/1B	37	70.0	73.6 ± 13.7	
13	94/06/30	21:21:10	S12E27	M2.5/1B	86	72.0	48.0 ± 4.0	(c)
14	94/08/14	17:36:31	S12W08	M3.9/1N	56	38.0	41.9 ± 11.6	

(a) No SXT observation.
(b) PFI offpointed.
(c) The latter half of the impulsive phase may be missing due to the entrance of the spacecraft into the South Atlantic Anomaly.
[1]Peak time in the M2-band count rate.
[2]M2-band peak count rate in units of counts/s/subcollimator.
[3]Duration of the impulsive phase (the period of time over which the analyzed double sources are seen).
[4]Corrected for foreshortening effects on the Sun.

$\Delta\gamma > 0$, *i.e.*, the corresponding hard X-ray spectrum breaks up toward lower energies at around 20 – 30 keV. On the other hand, events without separating footpoints tend to show a spectrum which breaks down toward lower energies ($\Delta\gamma < 0$). Hence this relationship can be summarized as:

$$v_{\rm sep} \gtrsim 0 \Longleftrightarrow \Delta\gamma \gtrsim 0 \ . \tag{2}$$

There is no systematic difference in $\gamma_{\rm M2/M1}$ between the two classes of events, with $\gamma_{\rm M2/M1}$ ranging in between 2 to 5 for both of the classes. On the other hand, whilst events with separating footpoints show $\gamma_{\rm M1/L} = 3 - 5$, events without separating footpoints systematically show harder spectra; $\gamma_{\rm M1/L} = 2 - 3.5$. This indicates that the observed difference in $\Delta\gamma$ between the two classes is mainly caused by spectral difference in the energy range below 20 – 30 keV.

2.3. Magnetic Field Configuration and Thermal/Non-Thermal Characteristics of Flares

We observe that the break up in hard X-ray spectra below 20 – 30 keV seen in events with separating footpoints is most likely caused by the presence of super-hot plasma, with temperature 30 – 50 MK (Lin *et al.* 1981), located at the top of the flaring loop. Figure 3 shows HXT images (in contours) of the 15 November 1991 and 10 November 1991 flares in the L- and M2-bands. For the 15 November 1991 flare, which shows separating footpoints, the L-band source differs in morphology from the M2-band sources; the latter represents loop footpoints while the former which has a softer spectrum than the footpoint sources is most likely originated from super-hot plasma located near the top of the loop. On the other hand, in the case of the 10 November 1991 flare, which lacks separating footpoints, double footpoint sources are clearly discernible even in the L-band without any additional sources. Such morphological characteristic is also found in the rest of the 14 events. We argue, from spectral and morphological considerations, that flares which show separating footpoints tend to produce super-hot plasmas near the top of the loop, while those without separating footpoints no, or little, such plasma is produced there during the impulsive phase.

Let us now discuss magnetic field configuration inferred from the separating/not-separating footpoints. The separating footpoints seen in seven events suggest a rising energy release (particle acceleration) site during the course of the flare. This behavior of the footpoints may support the loop-with-a-cusp magnetic field configuration where energy release via reconnection takes place at progressively higher altitudes, with outer field lines participating in the reconnection, which results in the systematic increase of separation between a pair of hard X-ray double footpoint sources. For events without separating footpoints, we argue that are caused by emerging-flux-type interaction in

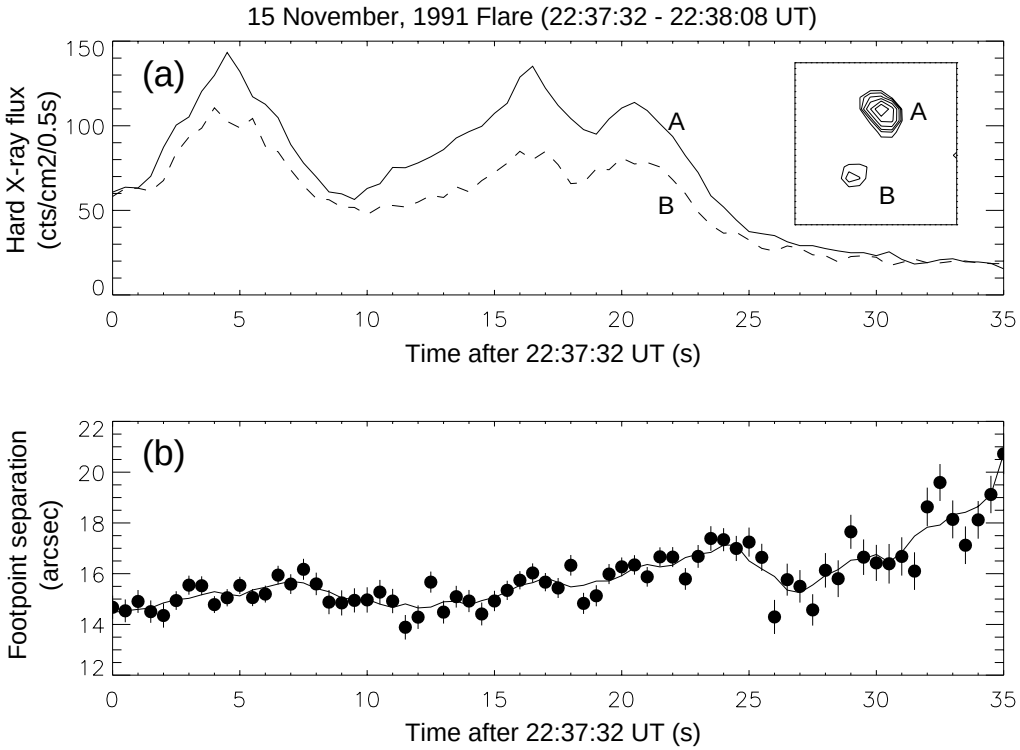

Fig. 1. Separating footpoints seen in the 15 November 1991 flare. (a) Time profiles of M2-band hard X-ray fluxes from the double sources A and B (shown in the inset). (b) Separation of the footpoints $s(t)$ (corrected for foreshortening effects) every 0.5 s. The solid line denotes a running average of $s(t)$ with a 2-second window. Error bar for each data point represents the 1σ statistical level. (After Sakao, Kosugi, and Masuda 1998.)

which a low-lying smaller loop interacts with an over-lying larger loop (Canfield *et al.* 1996; Hanaoka 1996, 1997; Nishio *et al.* 1997). If hard X-rays are to be emitted (by some reason) from the footpoints of the smaller loop, then newly reconnected field lines have smaller footpoint separation than the previous ones, which would result in decreasing, or at lease not increasing, footpoint separation (see Sakao, Kosugi, and Masuda (1998) for details of discussion).

By combining the inferred magnetic field configuration and spectral characteristics seen in the 14 events, we conjecture the following (Figure 4):

1. Two different magnetic field configurations, namely loop-with-a-cusp and emerging-flux-type, are responsible for energy release via magnetic reconnection in solar flares.

2. Electrons are accelerated in both of the two configurations while super-hot plasmas at the loop top are created if, and only if, the magnetic field has the loop-with-a-cusp configuration.

3. Hard X-ray spectra that break down toward lower energies at around 20 – 30 keV, which characterizes flares with the emerging-flux-type configuration, reflect bare non-thermal emission from the footpoints. In the meantime, spectra of flares with the loop-with-a-cusp configuration are composed of thermal emission from super-hot plasmas (with temperature 30 – 50 MK) and non-thermal emission, with the former being responsible for the spectral break-up toward lower energies.

4. Particle (electron) acceleration may take place at the reconnection site, *i.e.*, irrespective of the configuration of the surrounding magnetic fields. On the other hand, creation (and confinement) of super-hot plasmas during the impulsive phase is affected by the macroscopic field configuration.

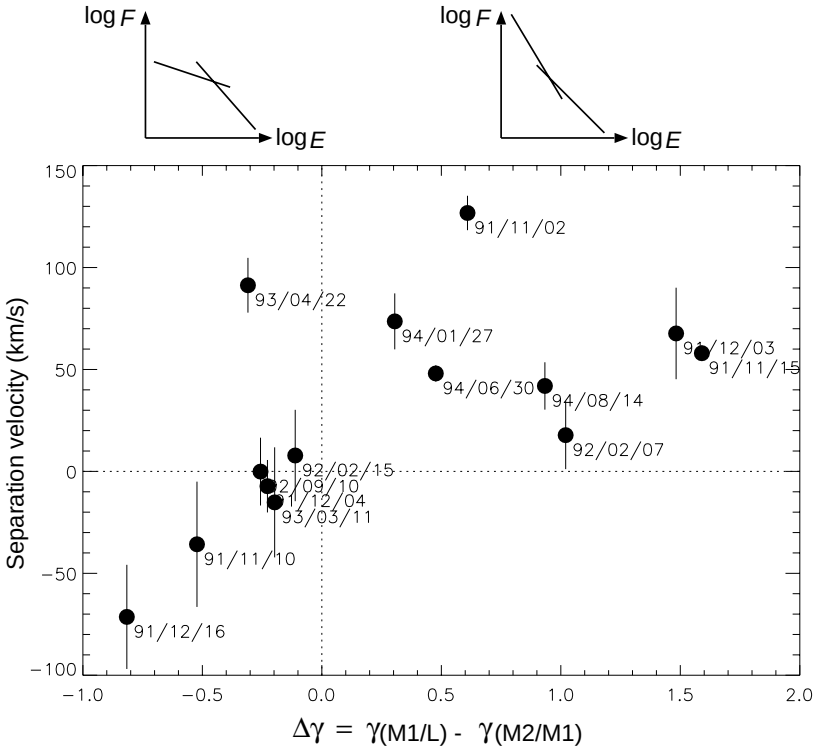

Fig. 2. Relationship between separation velocity $v_{\rm sep}$ of the double footpoint sources (corrected for foreshortening effects) and spectral shape of spatially-integrated hard X-rays. (After Sakao, Kosugi, and Masuda 1998.)

3. Electron Acceleration and the Global Magnetic Field Structure

3.1. Motions of Individual Footpoints

In the previous section, we concentrated on the separation of double footpoint sources and investigated its relationship with the creation of super-hot plasmas during the impulsive phase. We now turn to the individual motion of the double sources for events with separating footpoints. In the right panel of Figure 5 (a) we present trajectory of the centroid positions of the M2-band double sources for the 2 November 1991 flare (white dots), with the effect of spacecraft jitter removed. Accuracy of position determination for the centroids ranges in between $\pm$ (0.3″– 0.5″) at the 1σ level, depending on count statistics. During the impulsive phase, each of the footpoints tends to move toward a certain direction as indicated by arrows in the figure, showing a narrow and elongated trajectory. What is remarkable is that the footpoints do not separate along the line connecting the two; rather, they move nearly anti-parallel to each other with their overall separation increasing. Also, when we compare left and right panels of Figure 5 (a), we notice that at least one of the hard X-ray footpoints (north-eastern one) moves *along* the footpoint portion of the corresponding soft X-ray loop system.

Such behavior of the footpoints is also observed in other events. In the right panel of Figure 5 (b) we show another example, the 15 November 1991 flare, where each of the centroid positions of the footpoints again show systematic motion during the impulsive phase. Accuracy of the position determination is $\pm$ (0.3″ − 0.5″). Like in the 2 November 1991 flare, the separating footpoints move more or less anti-parallel to each other, with their overall separation increasing. Each of the footpoints also moves along the footpoint portion of the corresponding soft X-ray loop. It is worthwhile mentioning that in the case of this event, trajectory of the northern footpoint consists of two distinct (possibly three) "lines", with the footpoint moving from lower-right to upper-left direction along each of them as indicated by arrows in the panel. The first two lines in the trajectory correspond to two distinct spikes seen in the M2-band time profile (22:37:32 UT – 22:37:41 UT and 22:37:41 UT – 22:38:01 UT, respectively) shown in the inset. Such a trajectory may reflect three-dimensional evolution of the energy release site; not only the upward evolution, but also evolution in the horizontal direction parallel to the photosphere, with the two hard X-ray spikes

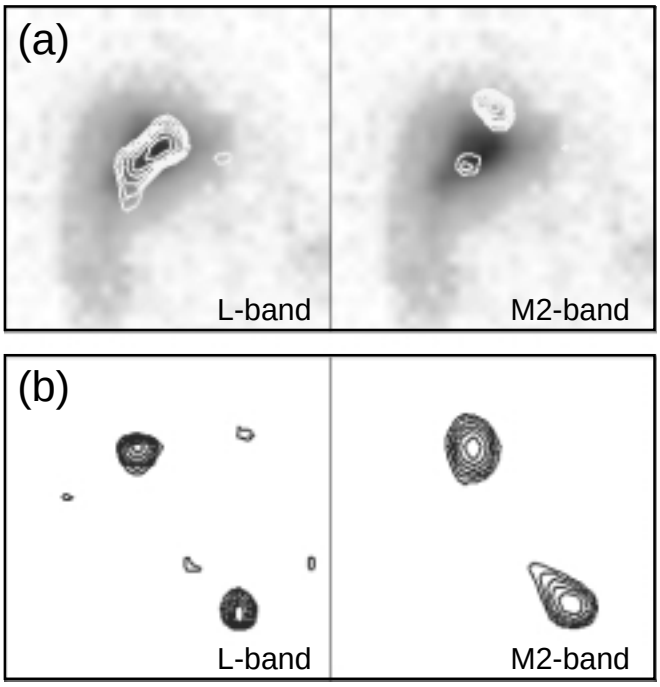

Fig. 3. Hard X-ray sources seen in the L- and M2-bands of HXT at the peak of emission in the M2-band (contours). (a) The 15 November 1991 flare (event 3 in Table 1) which shows separating footpoints. Soft X-ray image taken with the Be filter of SXT is overlaid on each map (grayscale). (b) The 10 November 1991 flare (event 2 in Table 1) which lacks separating footpoints. No SXT observation was made for this flare. The contour levels in each map are 70.7, 50.0, 35.4, 25.0, 17.7, and 12.5 % of the peak brightness. The field-of-view size of each map is $79'' \times 79''$. Solar north is to the top, east is to the left. (After Sakao, Kosugi, and Masuda 1998.)

possibly corresponding to the energy release site different horizontally in the magnetic field structure.

Motions of individual footpoints seen in the 7 events with increasing footpoint separation are briefly summarized as follows: (1) In all of the 7 events, at least one of a pair of footpoints shows systematic motion during the impulsive phase. The trajectory of such a footpoint tends to show, in 30 – 60 seconds, a narrow "line" (whose width $\lesssim$ 1,500 km) with its length typically ranging from 2,000 km to 5,000 km. (2) Hard X-ray double footpoints do not necessarily move in parallel (in the same direction), but rather in anti-parallel direction to each other (in 4 out of the 7 events; events 1, 3, 12, 13 in Table 1), with their overall separation increasing. Each of the footpoints tends to move not perpendicular to the neutral line, but rather parallel to it. Also, direction of the anti-parallel motion, when compared with the transverse component of photospheric magnetic field across the neutral line, suggests that the flaring hard X-ray loops have progressively smaller degree of shear with respect to the neutral line. (Comparison with magnetograms are not presented in this *manuscript*.) (3) The trajectory of (at least one of a pair of) hard X-ray double sources lies *along* the footpoint portions of a system of flaring soft X-ray loops (see Figure 5). Also, (4) for events where Hα images are available, at least one of a pair of double footpoints moves along the corresponding Hα ribbon, at its outermost edge, as indicated by the combination of Figure 5 (a) (right panel) and Figure 6 (a) for the north-eastern footpoint source of the 2 November 1991 flare.

While the separating footpoints tend to show systematic motion over a spatial scale of a few $\times 10^3$ km, events without separating footpoints do not show any systematic motion in their footpoint locations (except for the 10 September 1992 flare). In the following, we concentrate on the events with separating footpoints and discuss magnetic field structure inferred from their footpoint motions. Events without separating footpoints will be discussed in detail as a separate issue.

3.2. Three-Dimensional Magnetic Structure Inferred from Separating Hard X-ray Footpoints

We have seen that for events with separating footpoints, which suggest the loop-with-a-cusp magnetic field, hard X-ray footpoints show systematic motion during the impulsive phase. The footpoints do not separate along the line

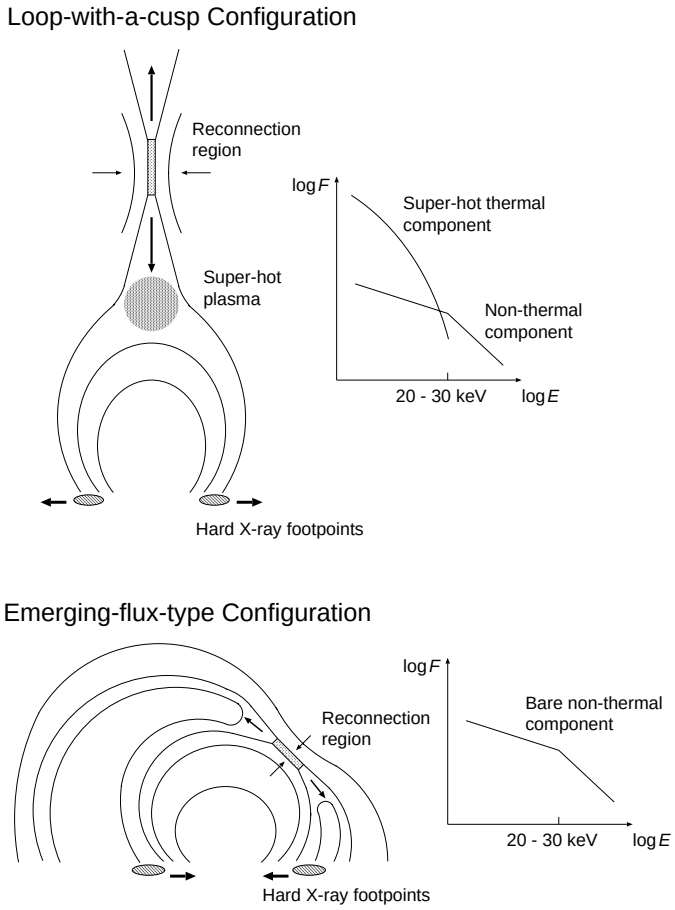

Fig. 4. Relationship between two-dimensional magnetic field configuration and thermal/non-thermal hard X-ray production in impulsive flares. Flares with the loop-with-a-cusp configuration tend to produce super-hot plasmas at the loop top while little such plasma is produced for flares with the emerging-flux-type configuration. (After Sakao, Kosugi, and Masuda 1998.)

connecting the two, but they most frequently move nearly anti-parallel to each other, showing a pair of elongated trajectories. Such motion of the footpoints may imply that the magnetic field structure for this type of events is comprised of an arcade, with a cusp structure at its ridge. The presence of such a magnetic arcade is further supported by the presence of a two ribbon structure seen in the corresponding Hα images. Furthermore, the anti-parallel motion of the hard X-ray footpoints and its relationship with the transverse component of the photospheric magnetic field suggests that reconnected field lines, along which accelerated electrons precipitate, may have progressively smaller shear angles for field lines with higher altitude. This indicates that longitudinal magnetic field component along the arcade axis needs be present at the reconnection site (*i.e.*, the magnetic field has a "sheared arcade" structure) and that the longitudinal component would progressively decrease as magnetic reconnection proceeds in this arcade structure with a rising reconnection site (Figure 7). A simple arcade without any such shear component would not be able to explain the observations; if magnetic reconnection were to proceed upwards or along the major axis of the arcade, then the double sources would simply separate along the line connecting the two or move parallel to each other in the same direction, respectively.

4. Perspective

4.1. Combined Investigation with Hα Data

In Figure 6 (a), we notice that the north-eastern hard X-ray source in the 2 November 1991 flare is located at the outermost edge of the corresponding Hα ribbon at the line center and that the eastern half of this source lies

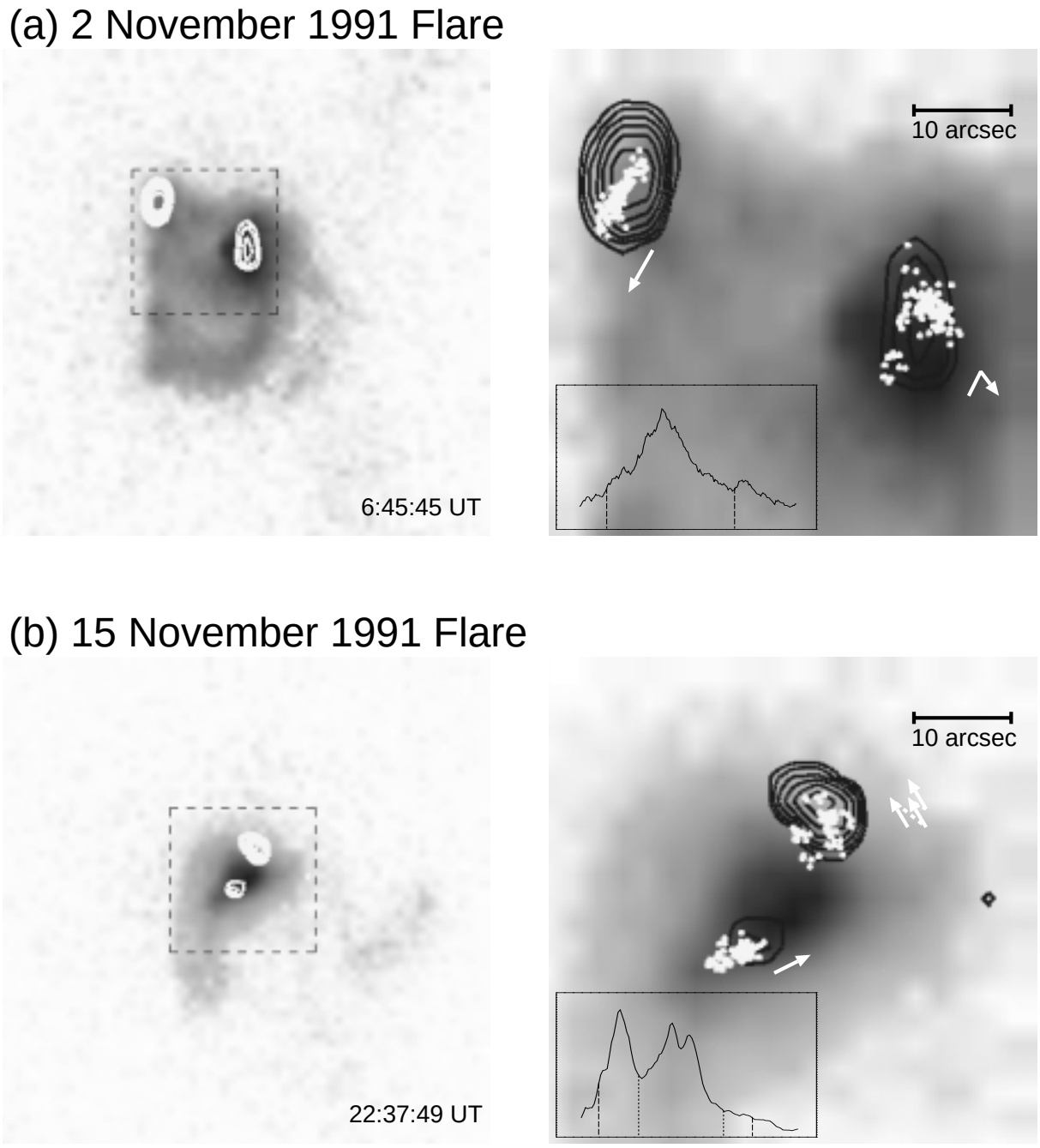

Fig. 5. (a) 2 November 1991 flare. *Left:* Hard X-ray double sources in the M2-band (white contours) at the peak of hard X-ray emission in the M2-band (at 6:45:45 UT) overlaid on a soft X-ray image taken with the Be filter of SXT at the corresponding time (negative grayscale). The box with dashed lines indicates the image area for the right panel. *Right:* Centroid positions of the double sources (white dots) in every 0.5 s from 6:45:20 UT to 6:46:19 UT, overlaid with the same hard and soft X-ray images in the left panel (black contours and negative grayscale, respectively). The M2-band time profile is shown in the inset, with the above-mentioned time interval indicated by dashed lines. (b) 15 November 1991 flare. *Left:* Hard and soft X-ray images (in the M2-band and with the Be filter, respectively), at the peak time of M2-band hard X-ray emission (22:37:49 UT). *Right:* Centroid positions of the double sources from 22:37:32 UT to 22:38:08 UT (white dots). Trajectory of the northern footpoint consists of two clearly-separated "lines", and possibly an additional one to the north-west of the two lines. The footpoint moves from lower-right to upper-left direction in each of the line, starting from the one nearest to the southern footpoint. The M2-band time profile is shown in the inset, with the above time interval shown in dashed lines. Dotted lines in the same inset indicate the timing where the location of the northern footpoint jumps from the upper-left edge to the lower-right edge of the next line in the trajectory. Note the jump from the first to the second line just corresponds to a valley seen in the hard X-ray time profile. For both of the flares, the effect of spacecraft jitter is removed, with typical accuracy for the determination of centroid positions $\sim \pm$ (0.3″– 0.5″) (at the 1σ level). Contour levels of hard X-ray sources in each of the four panels are 70.7, 50.0, 35.4, and 25.0 % of the peak brightness. Solar north is to the top, east is to the left.

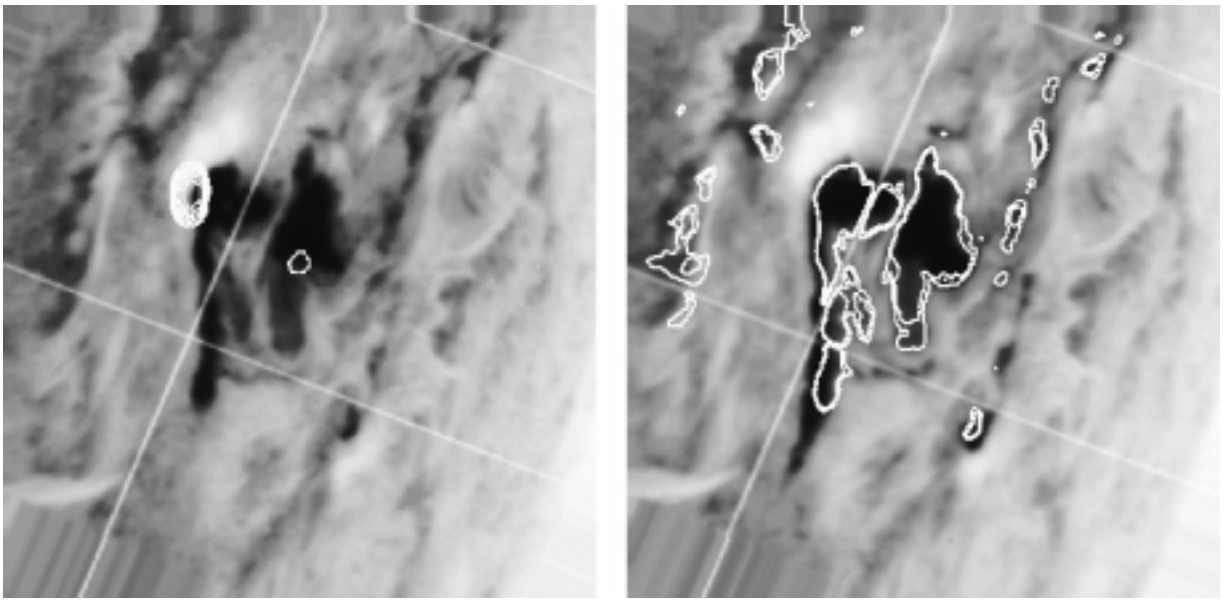

Fig. 6. Hard X-ray sources in the M2-band and the corresponding Hα (line center) images for the 2 November 1991 flare. *Left:* (a) Hard X-ray sources (contours) near the peak of hard X-ray emission (at 6:45:39 UT), overlaid on an Hα image (in negative grayscale) taken simultaneously at Hida Observatory, Kyoto University. Contour levels are 70.7, 50.0, 35.4, 25.0, 17.7, and 12.5 % of the peak brightness and the field-of-view size is $158'' \times 158''$. Hair cursors of the Hα telescope are seen as straight lines. Solar north is to the top, east to the left. *Right:* (b) Hα image taken at 6:48:46 UT (in negative grayscale) overlaid with the one at 6:45:39 UT (contours).

outside of the ribbon. Figure 6 (b) shows Hα images taken at 6:48:46 UT (negative grayscale) overlaid with the one at 6:45:34 UT (contours). We notice that, even at this time, Hα brightenings do not increase in area toward outside of the previously-existed ribbon around the footpoint. (A similar relationship between one of a pair of hard X-ray footpoints and Hα brightenings (at the line center) is also found for the 15 November 1991 flare (Wülser 1998).) This might imply that the apparent size ($\sim 6''$ FWHM in the east-west direction) of the hard X-ray source would be due to limited angular resolution of the HXT ($\sim 5''$); if the size of this source were to represent actual size of the area of electron precipitation, then we would expect that Hα brightenings would cover the entire hard X-ray source due to the heating of the chromosphere by precipitating electrons (*e.g.*, Canfield, R.C., Gunkler, T.A., and Ricchiazzi, P.J. 1984). The actual size of the source (site of electron precipitation) could be quite small, with its size, say, $\sim 1''$ (a few $\times\ 10^{16}$ cm^2 in area) and that the site of electron precipitation is located very close to (or just on) the outermost edge of the Hα ribbon.

There is another possibility that the offset between hard X-ray and Hα sources is caused by the difference in height between the two. While this possibility needs be examined in more detail in a subsequent study, we note such offset, *i.e.*, a hard X-ray footpoint source located half-outside of the Hα ribbon, is seen in at least two events examined here (2 November 1991 and 15 November 1991, and also 30 June 1994; see figure 5 (c) of Silva *et al.* 1997). We speculate that these footpoint hard X-ray emissions might be originated close in altitude, within at most a few $\times\ 10^3$ km, to the Hα emission. Otherwise it would be difficult to see such systematic offset among flares with different locations on the Sun and directions of Hα ribbons. On the other hand, Matsushita *et al.* (1992) have reported that the average height of M2-band hard X-ray sources is 7.7×10^3 km above flaring Hα sources, which seems significantly higher than what is suggested from the direct comparison of hard X-ray and Hα sources. Further investigation must be necessary for resolving this apparent mismatch.

Regarding the site of electron precipitation, it is noteworthy that Canfield and his colleagues (Canfield *et al.* 1991) have identified, by combining Hα spectroheliograms from Sacramento Peak Observatory and hard X-ray spectral data from *SMM* HXRBS for five flares, that the area of electron precipitation at the chromosphere is as small as $\sim 10^{17}$ cm^2, which in turn suggests large electron beam fluxes of $\sim 10^{12}$ ergs/s/cm^2 and large number density of beam electrons on the order of 10^{10} /cm^3, for all of the five events. In addition to this, Ichimoto and Kurokawa (1984) reported a red-shifted emission feature seen in Hα spectrograph images (presumably representing mass downflow

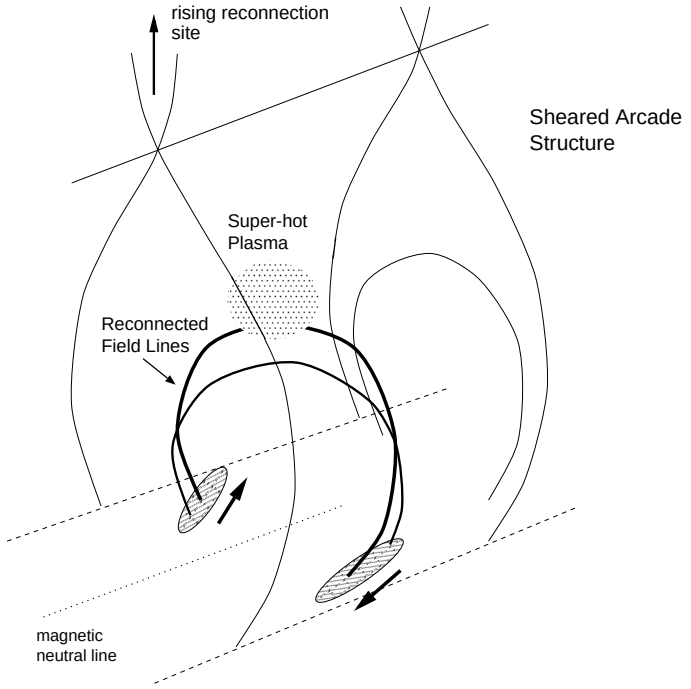

Fig. 7. Evolution of hard X-ray flaring loops (thick lines) and the global magnetic field structure inferred from the footpoint motions seen in flares with the loop-with-a-cusp configuration. X- (or Y-) type magnetic reconnection, which is responsible for the energy release, proceeds around the ridge of an arcade, at the tip of the cusp-shaped magnetic field. As the flare progresses, the reconnection site rises higher in the corona, resulting in the increase in the overall separation of the hard X-ray double footpoints. Due to the presence of longitudinal field component at the reconnection site, the successively-reconnected field lines would have different shear angles with each other, with respect to the photospheric magnetic neutral line. Such reconnected field lines, along which accelerated electrons precipitate downwards, are responsible for the anti-parallel motion of hard X-ray double footpoints (whose trajectory shown as hatched areas). Super-hot plasmas are created at the top of the hard X-ray loop(s) during the impulsive phase.

in the chromosphere caused by electron precipitation or by heat conduction from the corona) appears at the edge of an Hα ribbon in four flares observed at Hida Observatory. They further argued that this red-shifted feature is originated from a spatially confined region whose typical size is less than $1''$, with the region changing its location successively as the flare progresses.

These observations provide a very important piece of information in studying relationship between acceleration/precipitation of electrons and the flaring magnetic field structure. Now that we can identify sites of electron precipitation directly with hard X-ray images, comparison with Hα images and spectra will certainly give us valuable information on this issue. As shown in Figures 5 and 6, hard X-ray footpoint sources appear only in very limited portions of the corresponding soft X-ray/Hα loop system, suggesting that electron acceleration takes place in highly-confined region(s) in the global magnetic field structure. This, in turn, indicates that physical conditions necessary for the acceleration of electrons are quite hard to be realized and/or the acceleration requires particular configuration of magnetic field which can only be set up in a localized region in the overall flaring magnetic field. While the appearance of hard X-ray double footpoints itself suggests potential difficulty in the occurrence of electron acceleration, still the acceleration does take place (as indicated by non-thermal hard X-ray and microwave emissions) in most, if not all, flares. At present, it remains unanswered why acceleration of electrons in solar flares, which is inherently a microscopic plasma process, needs be accompanied with a large-scale magnetic field structure (see, *e.g.*, discussions in Miller *et al.* 1997). The separator/separatrix approach, which deals, by use of photospheric magnetic field data, with topological configuration of coronal magnetic field and its relationship with chromospheric/coronal signatures of flares (Gorbachev and Somov 1988; Den and Somov 1989; Longcope 1996), may be a promising method for investigating such problems.

4.2. Evolution of Active Regions, Energy Storage, and Hard X-ray Signatures of Flares

When we recall the relationship between separating/not-separating footpoints and the thermal/non-thermal characteristics of flares, it is likely that flares with sheared magnetic arcades tend to produce super-hot plasmas at the loop top during the impulsive phase. Although the mechanism for this association is not yet identified, it is suggestive that Falconer *et al.* (1997) demonstrated that sites in active regions which are persistently bright in soft X-rays (without flares) are preferentially associated with strongly-sheared portions of photospheric neutral lines. This may indicate a possibility that (strong) heating of coronal plasmas is accompanied closely with sheared magnetic field and that flares which commence with such magnetic field structure also exhibit strong heating of plasmas to 30 – 50 MK; *i.e.*, evolution of active regions itself might characterize thermal aspect of flares.

An interesting approach to this issue has recently been attempted by Saita (1998) and Saita *et al.* (1999). By choosing several active regions that produced a number of flares observed with HXT, they have investigated evolution of photospheric magnetic field in a time scale of days around the site of flares and its relationship with spectral hardness of the flares (below 20 – 30 keV). They found that events with hard spectra ($\gamma_{\mathrm{M1/L}} \lesssim 4$ at the peak of hard X-ray emission) tend to commence at sites where either of the positive or negative polarity regions gradually intrude into the other, increasing complexity of the neutral line profile. Also, weak transverse magnetic field is associated with these sites, showing little magnetic shear across the neutral line. They have also shown that in active regions whose flaring activities were identified by Hanaoka (1997) as due to flux emergence, flares tend to exhibit hard spectra (with $\gamma_{\mathrm{M1/L}} \lesssim 4$). This may suggest that the above-mentioned evolution of photospheric magnetic field could be caused by the emergence of new magnetic fluxes, although further confirmation is necessary. On the other hand, in active regions where the associated hard X-ray events have shown soft spectra below 20 – 30 keV ($\gamma_{\mathrm{M1/L}} \gtrsim 4$), which possibly indicates the presence of super-hot plasmas at the loop top, each site of flares has accompanied a neutral line which decreases complexity of its profile as the active region develops (see Figure 8). Also, such a neutral line is accompanied with well-developed, sheared transverse magnetic field component, which signifies a site that preferentially produces major flares (Moore, Hagyard, and Davis 1987; Hagyard, Venkatakrishnan, and Smith 1990).

The observations presented here may give us some hints for a possible relationship between the development of active regions, associated energy storage in the corona, and hard X-ray signatures of flares under certain magnetic field configuration resulted from that development. One question that we have to bear in mind when considering such a relationship is the role of flux emergence. While it is widely recognized that there is close association of emerging-flux activities with the occurrence of flares (Kurokawa 1989), we have not yet understood how it is related to the storage and release of magnetic energy in the corona, which leads to flares. Flux emergence may directly trigger flares (by directly interacting with overlying coronal magnetic field), or it may serve as an agent for accumulating magnetic energy into the corona whose photospheric manifestation observed as "flux cancellation" (Zwaan 1987; van Ballegooijen and Martens 1989; Martin and Livi 1992) while some other possibilities may also exist. Detailed studies on the evolution of photospheric magnetic field in combination with that of coronal structure seen in X-rays, which is a part of scientific objectives of the next Japanese mission *Solar-B*, should provide clues to these mechanisms.

We would like to express our sincere gratitude to ISAS, NASA, SERC, and the *Yohkoh* Team for their continuous support to the mission. We owe our thanks to Prof. H. Kurokawa and Dr. R. Kitai of Hida Observatory, Kyoto University, for providing Hα images for the 2 November 1991 event. We also greatly appreciate Dr. J.-P. Wülser of Lockheed Martin Advanced Technology Center for providing us with Hα data of the 15 November 1991 flare taken at the Mees Solar Observatory, University of Hawaii, as well as for valuable discussions. Ms. N. Saita is appreciated for providing the drawing for Figure 8. This work is partially supported by the Scientific Research Fund of the Ministry of Education, Science and Culture under Grant No. 08304021 and No. 09640327.

References

Canfield, R.C., Gunkler, T.A., and Ricchiazzi, P.J., *Astrophys. J.*, **282**, 296 (1984).
Canfield, R.C., Zarro, D.M., Wülser, J.-P., and Dennis, B.R., *Astrophys. J.*, **367**, 671 (1991).
Canfield, R.C., Reardon, K.P., Leka, K.D., Shibata, K., Yokoyama, T., and Shimojo, M., *Astrophys. J.*, **464**, 1016 (1996).
Den, O.G., and Somov, B.V., *Astron. Zh.*, **66**, 294 (1989) in Russian; also *Sov. Astron.*, **33**, 149 (1989) in English.
Falconer, D.A., Moore, R.L., Porter, J.G., Gary, G.A., and Shimizu, T., *Astrophys. J.*, **482**, 519 (1997).
Forbes, T.G., and Malherbe, J.M., *Solar Phys.*, **135**, 361 (1991).
Gorbachev, V.S., and Somov, B.V., *Solar Phys.*, **117**, 77 (1988).
Hagyard, M.J., Venkatakrishnan, P., and Smith, Jr., J.B., *Astrophys. J. Suppl.*, **73**, 159 (1990).

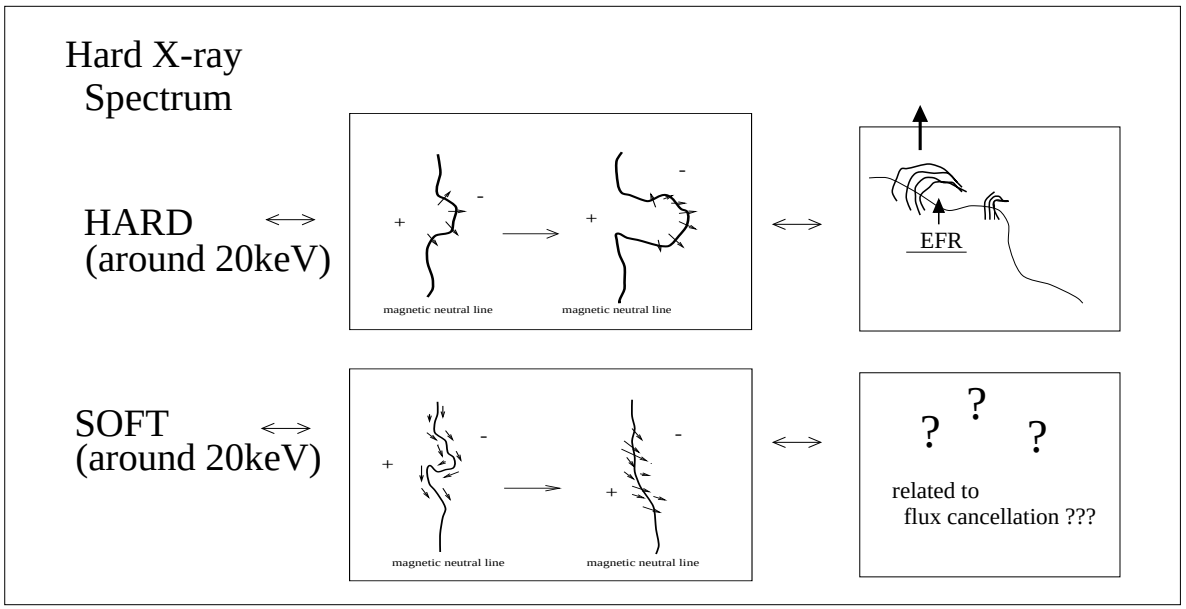

Fig. 8. A diagram which schematically illustrates relationship between the evolution of photospheric magnetic field with a time scale of days and hard X-ray spectral characteristics of flares which commence in association with that evolution. (After Saita 1998.)

Hanaoka, Y., *Solar Phys.*, **165**, 275 (1996).
Hanaoka, Y., *Solar Phys.*, **173**, 319 (1997).
Hirayama, T., *Solar Phys.*, **34**, 323 (1974).
Ichimoto, K., and Kurokawa, H., *Solar Phys.*, **93**, 105 (1984).
Kopp, R.A., and Pneuman, G.W., *Solar Phys.*, **50**, 85 (1976).
Kosugi, T., Makishima, K., Murakami, T., Sakao, T., Dotani, T., Inda, M., Kai, K., Masuda, S., Nakajima, H., Ogawara, Y., Sawa, M., and Shibasaki, K., *Solar Phys.*, **136**, 17 (1991).
Kosugi, T., Sakao, T., Masuda, S., Makishima, K., Inda, M., Murakami, T., Ogawara, Y., Yaji, K., and Matsushita, K., *Publ. Astron. Soc. Japan*, **44**, L45 (1992).
Kosugi, T., in *High Energy Solar Physics*, AIP Conf. Proc. 374, eds. Ramaty, R., Mandzhavidze, N., and Hua, X.-M. p. 267 (1996).
Kurokawa, H., *Sp. Sci. Rev.*, **51**, 49 (1989).
Lin, R.P., Schwartz, R.A., Pelling, R.M., and Hurley, K.C., *Astrophys. J. Lett.*, **251**, L109 (1981).
Longcope, D.W., *Solar Phys.*, **169**, 91 (1996).
Martin, S.F., and Livi, S.H.B, in *Eruptive Solar Flares*, Lecture Notes in Physics 399, eds. Švestka, Z., Jackson, B.V., and Machado, M.E., Springer, p. 33 (1992).
Matsushita, K., Masuda, S., Kosugi, T., Inda, M., and Yaji, K., *Publ. Astron. Soc. Japan*, **44**, L89 (1992).
Masuda, S., Ph.D. Thesis, The University of Tokyo (1994).
Masuda, S., Kosugi, T., Hara, H., Tsuneta, S., and Ogawara, Y., *Nature*, **371**, 495 (1994).
Masuda, S., Kosugi, T., Hara, H., Sakao, T., Shibata, K., and Tsuneta, S., *Publ. Astron. Soc. Japan*, **47**, 677 (1995).
Miller, J.A., Cargill, P.J., Emslie, A.G., Holman, G.D., Dennis, B.R., LaRosa, T.N., Winglee, R.M., Benka, S.G., and Tsuneta, S., *J. Geophys. Res.*, **102**, 14631 (1997).
Moore, R.L., Hagyard, M.J., and Davis, J.M., *Solar Phys.*, **113**, 347 (1987).
Nishio, M., Yaji, K., Kosugi, T., Nakajima, H., and Sakurai, T., *Astrophys. J.*, **489**, 976 (1997).
Saita, N., Master Thesis (in Japanese), Rikkyo University (1998).
Saita, N., *et al.*, in preparation (1999).
Sakao, T., Ph.D. Thesis, The University of Tokyo (1994).
Sakao, T., Kosugi, T., and Masuda, S., in *Observational Plasma Astrophysics: Five Years of Yohkoh and Beyond*, eds. Watanabe, T., Kosugi, T., and Sterling, A.C., Kluwer, p. 273 (1998).
Schmieder, B., Forbes, T.G., Malherbe, J.M., and Machado, M.E., *Astrophys. J.*, **317**, 956 (1987).
Silva, A.V.R., Wang, H., Gary, D.E., Nitta, N., and Zirin, H., *Astrophys. J.*, **481**, 978 (1997).
Švestka, Z.F., Fontenla, J.M., Machado, M.E., Martin, S.F., Neidig, D.F., and Poletto, G., *Solar Phys.*, **108**, 237 (1987).

Tsuneta, S., Acton, L., Bruner, M., Lemen, J., Brown, W., Caravalho, R., Catura, R., Freeland, S., Jurcevich, B., Morrison, M., Ogawara, Y., Hirayama, T., and Owens, J., *Solar Phys.*, **136**, 37 (1991).

Tsuneta, S., Hara, H., Shimizu, T., Acton, L.W., Strong, K.T., Hudson, H.S., and Ogawara, Y., *Publ. Astron. Soc. Japan*, **44**, L63 (1992a).

Tsuneta, S., Takahashi, T., Acton, L.W., Bruner, M.E., Harvey, K.L., and Ogawara, Y., *ibid.*, L211 (1992b).

van Ballegooijen, A.A., and Martens, P.C.H., *Astrophys. J.*, **343**, 971 (1989).

Wülser, J.-P., private communication (1998).

Zwaan, C., *Ann. Rev. Astron. Astrophys.*, **25**, 83 (1987).